

# Solving rescheduling problems in heterogeneous urban railway networks using hybrid quantum-classical approach

Mátyás Koniorczyk <sup>1</sup>, Krzysztof Krawiec <sup>2</sup>, Ludmila Botelho <sup>3 4</sup>, Nikola Bešinović <sup>5</sup>, Krzysztof Domino <sup>3</sup>

<sup>1</sup> HUN-REN Wigner Research Centre for Physics, Konkoly-Thege Miklós út 29-33., Budapest, 1121, Hungary

<sup>2</sup> Faculty of Transport and Aviation Engineering, Silesian University of Technology, Akademicka 2A, Gliwice, 44-100, Poland

<sup>3</sup> Institute of Theoretical and Applied Informatics, Polish Academy of Sciences, Bałycka 5, Gliwice, 44-100, Poland

<sup>4</sup> Joint Doctoral School, Silesian University of Technology, Akademicka 2A, Gliwice, 44-100, Poland

<sup>5</sup> “Friedrich List” Faculty of Transport and Traffic Sciences, Technical University of Dresden, Dresden, 01069, Germany

E-mail: [konioczyk.matyas@wigner.hun-ren.hu](mailto:konioczyk.matyas@wigner.hun-ren.hu), [krzysztof.krawiec@polsl.pl](mailto:krzysztof.krawiec@polsl.pl), [lbotelho@iitis.pl](mailto:lbotelho@iitis.pl), [nikola.besinovic@tu-dresden.de](mailto:nikola.besinovic@tu-dresden.de), [kdomino@iitis.pl](mailto:kdomino@iitis.pl)

## Abstract

We address the applicability of hybrid quantum-classical heuristics for practical railway rescheduling management problems. We build an integer linear model for the given problem and solve it with D-Wave’s quantum-classical hybrid solver as well as with CPLEX for comparison. The proposed approach is demonstrated on a real-life heterogeneous urban network in Poland, including both single- and multi-track segments and covers all the requirements posed by the operator of the network. The computational results demonstrate the readiness for application and benefits of quantum-classical hybrid solvers in the realistic railway scenario: they yield acceptable solutions on time, which is a critical requirement in a rescheduling situation. At the same time, the solutions that were obtained were feasible. Moreover, though they are probabilistic (heuristics) they offer a valid alternative by returning a range of possible solutions the dispatcher can choose from. And, most importantly, they outperform classical solvers in some cases.

## Keywords

railway rescheduling, conflict management, heterogeneous urban railway network, quantum annealing, hybrid quantum-classical heuristics

## 1 Introduction

Rail transport is expected to experience an increase in capacity demands due to changes in mobility needs resulting from climate policy, leading to traffic challenges in passenger and cargo rail transport. The situation is aggravated by the fact that the rolling stock and especially railway infrastructure cannot keep up with the increase in transport needs, which overloads railway systems. Rail transport, due to its technical and organizational characteristics is very sensitive to disturbances and disruptions in traffic: these extraordinary events have an impact on railway operations, typically resulting in delays (Ge et al., 2022). Examples of such disturbances include: late train departures/arrivals, extended dwell times. These can last from several minutes up to hours. A *disturbance* is a smaller perturbation that can be handled solely by modifying the existing train paths, whereas a disruption affects rolling stock and crew schedules, too (Cacchiani et al., 2014). In the present work we focus on rescheduling of trains, which is the network operator’s perspective, even though we also consider (partial) track closures, which are typically considered as disruptions. In our examples, however they will be managed by modifying existing train paths. The impact of disturbances and disruptions can propagate to multiple sections in the railway network (c.f. Törnquist (2007) and references therein). Thus, ensuring stable railway traffic and providing reliable service for passengers, rail cargo companies, and their clients is in the best common interest of railway infrastructure managers, and train operators.

As a railway network is a complex non-local structure, modeling a bigger portion of it is necessary for efficient suppression of the consequences of disturbances. While doing so, diverse objective functions were addressed, such as the (weighted) sum of delays (Lange and Werner, 2018), the maximal delay that cannot be avoided (D’Ariano et al., 2007), or fuel consumption measures (Harrod, 2011). Large-scale rescheduling problems have to be addressed, and as the time available for making decisions is limited, they have to be solved almost real time. The railway dispatching/rescheduling problem is recognized as equivalent to job-shop scheduling with blocking and no-wait constraints (Szigel, 1973; Mascis and Pacciarelli, 2002). It has an extensive literature, already summarized in a number of reviews, including those by Cacchiani et al. (2014), by Lamorgese et al. (2018), or by Philip and Swapnesh (2022).

The maybe most frequently applied modeling strategy is based on alternative graphs (D’Ariano et al., 2007; Mascis and Pacciarelli, 2002) which can be formulated as a mixed integer linear program, often referred to as the big-M model. As this model often becomes too big to be solved on time, a number of strategies are applied, including heuristics, specific branch-and-bound methods, alternative formulations, decompositions, and the combinations of these; see the work of Lamorgese et al. (2018) for a review of the model and the methods.

An alternative approach is to use time-indexed models: discrete-time units and binary decision variables that assign events to particular time instants. Even though this results in very large problems, it is applied for both timetabling and dispatching/rescheduling (Caimi et al., 2012; Lusby et al., 2013; Meng and Zhou, 2014). As this approach results in a 0 – 1 program, which is promising when one considers the use of 0 – 1 solvers such as quantum hardware. Indeed, job-shop problems addressed on pure quantum hardware (Venturelli et al., 2015), and even in certain hybrid approaches (Kurowski et al., 2020) use similar models, and our previous work (Domino et al., 2023) which was the first to apply a quantum solver to railway dispatching problems also followed this route. In the present work, however, we deal with a variant of the big-M model, albeit with discrete time variables, resulting in an integer linear program (ILP). We introduce a variant of this type of model which maintains a reasonable model size while addressing practically relevant problem instances. In this way, a hybrid classical-quantum integer solver can be applied to solve them, and a comparison with a classical solver is also possible.

In particular, we address the train rescheduling problem in complex railway networks with mixed infrastructure including single, double, and multiple-track railway lines with given planned train paths. Our consideration includes shunting movement of rolling stock between depots and stations followed by rolling stock connections. We apply a new hybrid rescheduling algorithm combining classical-quantum modeling and based on Quantum Annealing (QA). This work extends on a particular linear modeling strategy, partly explored on a toy model by Domino et al. (2022b). Our (ILP) model, tailored for the particular practical railway situation, is solved with proprietary D-Wave solvers as well as with CPLEX for comparison.

We recognize several important scientific gaps. First, existing optimization models suffer from the curse of dimensionality, and inability to solve larger real-life instances. Second, the QA models for the studied optimization problem that have been introduced so far had been designed for pure QA implementations and have been demonstrated only on simple network setups due to the size limitations of the currently available Noisy Intermediate Scale Quantum (NISQ) devices. Third, no hybrid QA-based models have been used for real-life railway, or even other schedule-based modes, like public transport and air traffic planning and/or rescheduling. In this paper we demonstrate the quantum readiness of medium-scale railway rescheduling models: we successfully apply quantum methods in the rescheduling problem of a urban railway networks.

The paper is organized as follows. In Section 2 we briefly review state-of-the-art of quantum annealing and its applications. In Section 3 we describe problem under investigation, in Section 4 we evaluate our model, in Section 5 we discuss the hybrid solver we use, in Section 6 we present computational results.

## 2 Quantum annealing

Quantum computing devices became available for practical computational purposes in the last few years. Quantum annealers are such devices: they implement two-level quantum systems (quantum bits) with tunable pairwise interactions: an Ising system well-known in physics (Ising, 1925; Bian et al., 2010). The expression of the energy of such a system is one of the many equivalent forms of quadratic unconstrained binary optimization problems (QUBOs): the extremum of a quadratic function of binary variables, which is an NP-hard problem in general.

Hence, a QUBO objective can be expressed as the energy of the Ising system: the configuration of the pairwise couplings of the spins and the applied local fields, which are tunable in quantum hardware.

According to the adiabatic theorem of quantum mechanics (Avron and Elgart, 1999), tuning the system's configuration from a suitably chosen initial state to the one corresponding to the actual objective slowly enough, under certain conditions the optimal configuration can be read out. Unfortunately, not all QUBOs meet the required conditions, so even in an ideal setting the quantum annealer is not a universal solver of hard problems, but it can be efficient in certain problems. Quantum annealing can be also viewed as a process analogous to simulated annealing, in which the noise required to avoid staying in local optima has quantum (as opposed to thermal) origins (Das and Chakrabarti, 2008).

In real physical hardware, like the D-Wave machine, thermal noise and imperfections cannot be avoided, hence, the physical devices realize a combination of thermal and quantum annealing, which renders them a probabilistic heuristic solver for QUBOs. They output a number of configurations typically close to, and optionally including the optimal one.

The class of QUBO problems is well studied and have a number of applications; we refer the reader to a recent monograph edited by Punnen (2022). Linear unconstrained binary problems can also be considered as a special case of QUBOs, while linear and quadratic constraints can be taken into account with penalties (Gusmeroli et al., 2022). Using appropriate binary encoding of the variables, integer programming problems can also be treated. Hence, an efficient QUBO solver can be useful in many problems, including the integer linear programs arising in the present contribution.

The state-of-the-art physical quantum annealers are smaller systems of a few hundred quantum bits and not all pairs are coupled. The fixed topology of qubit couplings means that the problem's graph defined by the nonzero coupling has to be embedded as an induced subgraph of the topology of the system. This embedding is a hard problem itself (Zbinden et al., 2020). It often requires to couple multiple physical qubits to represent a logical bit of the problem. As quantum annealers are not algorithms running on digital computers but analog devices implemented physically, the coefficients of the problem are encoded with a limited accuracy.

To overcome the problem of limited size and accuracy, quantum annealers of the present state of the art are often used in hybrid (quantum-classical) solvers, orchestrating classical algorithms and using QA as a subroutine in order to address hard problem instances more efficiently. Solvers available in D-Wave's 'Leap Hybrid Solver Service (HSS)' (D-Wave Quantum Inc., 2022a), including the one used in the present work, belong to this family. Meanwhile, quantum technology keeps on developing, systems of bigger size and better topology are regularly announced, they are more and more affordable, and there is a growing community around them.

Currently, the applicability of QA technologies is being explored. In the railway context, the first applications of QA can be found in train dispatching/rescheduling (Domino et al., 2022b) and rolling stock planning (Bickert et al., 2021). In particular, the first proof-of-concept demonstration of a (pure) quantum computing approach to railway rescheduling was presented by some of us (Domino et al., 2023). A follow-up paper (Domino et al., 2022b) laid down the principles of a more general modeling approach to railway rescheduling in light of QA, introducing a suitable QUBO / HOBO (Higher-Order Binary Optimization) encoding of these problems. The present work continues this line of research, which is gaining increasing attention, e.g. the recent work of Xu et al. (2023).

### 3 Problem description

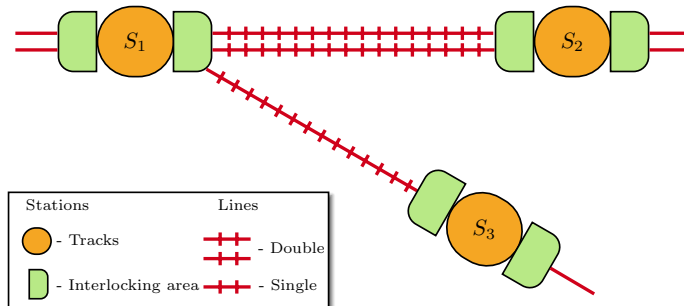


Figure 1: Edges and nodes on the example railway network. Interlocking areas of stations in green.

We consider a railway rescheduling problem that includes train reordering, retiming, and shunting

movements with rolling stock circulation at stations. Also, we consider an urban railway network with mixed tracks from single, double, to quadruple tracks.

We model a railway network with edges and nodes of a graph. Figure 1 depicts an exemplary network layout composed of nodes (station or junction) and edges (single, double, multiple-track lines). Each edge is composed of one or more *tracks*. Each track consists of block sections defined by pairs of signals (Lusby et al., 2013). Each block section can be occupied by at most one train at a time. A subsequent train is allowed to enter the block only after a minimal *headway*: minimal time span between the trains. We assume a 2-block signaling system, meaning that two free blocks are required between the consecutive trains. We also assume a green way policy (trains have the free way to move at the maximal allowed speed between stations), resulting in constant running times for each block.

Each node is composed of station tracks (blocks) and interlocking areas. One station track can be occupied by one train at a time. Routing dependencies between pairs of trains competing for the same resource in interlocking areas are considered to guarantee that only one train from the pair can occupy the area at the time.

A train’s *route* is the sequence of blocks the train passes during its journey. A train *path* is a sequence of arrival and departure times of a particular train assigned to a train route. We assume a one-minute resolution for all time parameters such as timetable time, running and dwell time minimal headway time, or passing time, resulting in integer variables. This assumption of discretized time is needed to enable the use of quantum-based solvers, and, more importantly, introduces the possibility of pruning the inherently binary variables. The relaxation of integer constraints on time variables is not expected to improve computation time significantly, as the real difficulty is tied to the precedence of trains, encoded later on precedence binary variables.

In the network, two trains can follow each other, i.e. keep the given order, meet and pass (M-P) when going the opposite directions, and meet and overtake (M-O), i.e. change the order, when going the same direction. Single-track lines are designed for bidirectional traffic, double track lines for unidirectional, one for each direction, and *multi-track* lines can be a combination of unidirectional and bidirectional. On *single-track* lines, M-Ps and M-Os are only possible at stations. To prevent M-P on single-track lines, we determine the set  $\mathcal{J}_{\text{single}}^2$  as the set of all pairs of trains that can potentially meet on the single-track line heading in opposite directions.

Trains in the same direction preserve their order between stations, and keep the minimal headway time between each other. To prescribe these we determine set  $\mathcal{J}_{\text{headway}}^2$ : the set of all pairs of trains that can potentially violate the minimal headway condition.

The train traffic is scheduled based on the given timetable. The timetable contains all the train paths. In the train rescheduling problem, we are given an initial timetable that is conflict-free. However, conflicts may appear due to disturbances such as late departures and/or arrivals due to excessive passenger demand, malfunctioning rolling stock, etc. Following Corman et al. (2012), a *conflict* is an inadmissible situation when at least a pair of trains claim the same resource (e.g., block section, switch) simultaneously. We assume that the conflict may occur either on the railway line or at the station. Possible conflicts that can occur on the line include the lack of the minimum headway between two subsequent trains heading on the same track in the same direction, or claiming a segment of a single-track line by two trains heading in opposite directions at the same time. Conflicts at stations include claiming a station track by two trains at the same time, or claiming a station switch (in the interlocking area) by two trains at the same time.

The conflicts have to be solved by modifying the original timetable, applying decisions on the train sequencing, and retiming for trains claiming the same resource. Such an intervention in the structure of train paths implies additional changes to maintain the feasibility of the modified timetable. These changes typically result in delays of additional trains that were not directly involved in the conflict otherwise, giving rise to *secondary delays* depending on the dispatching decision depending on the modification of the timetable. We will minimize a function of these secondary delays.

An important element of our approach is that from among all stations, we first determine a subset of the *decision stations*; we assume that the direct decisions implied by our model affect these stations only. Hence, as decision stations, we select those stations, where routes of trains intersect, where trains start or terminate, or where the selected part of the network is bounded. The motivation is that if the routes of trains are fixed, the decisions on modifying their train paths have to be made with respect to these stations. (If we change some of the trains’ routes in a re-routing process, the new model with new parameters is developed, e.g. additional decision stations may appear.) In what follows, by a station we always mean a decision station. This also means that non-decision stations appear only through the parameter values in the model,

they do not appear as indices of decision variables or parameters. Headways, for instance, are calculated between decision stations, taking into account all the line blocks and station blocks of non-decision stations in between.

On the station where a train terminates or sets off, shunting is also modeled. The goal of shunting is to move the train from the passengers' service track to the depot or vice versa. The depot is treated as the station, and consider it as a black box, without a detailed layout. We treat shunting movements as a service train from the depot to the starting station of the service train, or from the terminating station to the depot. The rolling stock circulation condition is applied to ensure the precedence between the service train and the actual train.

In this way our model shares features of both microscopic and macroscopic models. At the *decision stations* it is microscopic as it takes into account station technology, track occupancy, rolling stock circulation, and shunting. Meanwhile from the point of view of the rest of the network it is a macroscopic model.

## 4 Methods and Model

In the following, we describe our model in detail. Section 4.1 defines sets, parameters, and decision variables. Section 4.2 describes our Integer Linear Programming (ILP) formulation.

### 4.1 Sets, parameters and decisions

To formulate our decision variables, constraints, and the objective function, we determine sets of index tuples needed to find the actual index sets of variables, from the given infrastructure data, timetable data, and the rolling stock circulation plan. Also, we introduce parameters calculated from the same input.

#### Sets

Let us denote by  $\hat{S}$  the set of all stations, and by  $S \subset \hat{S}$  the decision stations we have determined in advance, as already described. The main objects of our model for railway rescheduling are the trains  $j \in \mathcal{J}$  and the stations  $s \in \mathcal{S}_j$  in their path. Set  $\mathcal{S}_j$  includes decision stations only and it is an ordered set. In addition to  $\mathcal{J}$  and  $\mathcal{S}_j$ , the relevant sets are the following. Set  $\mathcal{J}_s^{2(\text{turn})} \subset \mathcal{J} \times \mathcal{J} (\forall s \in S)$  is the set of all pairs of trains so that the first train of the pair terminates at station  $s$  and its rolling stock continues as the second train of the pair. This set is deduced from the rolling stock circulation plan and the timetable. Set  $\mathcal{J}^{2(\text{close})} \subset \mathcal{J} \times \mathcal{J}$  is the set of trains that are close enough to each other in time so that precedence variables have to be defined for them. More details will be given in the description of the parameter  $d_{\max}$  which this set depends on. Set  $\mathcal{J}^{2(\text{headway})} \subset \mathcal{J}^{2(\text{close})}$  is the set of train pairs that can potentially violate the minimal headway time between two subsequent trains on a line segment. For a pair of trains to be in  $\mathcal{J}^{2(\text{headway})}$ , both their routes need to include the same line segment so that the trains are moving in the same direction on it and can meet there according to model parameters, i.e. maximal allowed delay. Set  $\mathcal{J}^{2(\text{single})} \subset \mathcal{J}^{2(\text{close})}$  is the set of all trains that share at least one single-track line segment as a common part of their routes so that they are heading in the opposite direction. Set  $(\forall s \in S) \mathcal{J}_s^{2(\text{track})} \subset \mathcal{J}^{2(\text{close})}$  is the set of train pairs that are planned to occupy the same track on station  $s$  anytime during the planning horizon, thereby competing for the same track. Set  $(\forall s \in S) \mathcal{J}_s^{2(\text{switch,out})} \subset \mathcal{J}^{2(\text{close})}$  is the set of train pairs that are planned to pass the same interlocking area of  $s$  upon their departure from station  $s$ . Set  $(\forall (s, s') \in S \times S) \mathcal{J}_{s,s'}^{2(\text{switch,out,in})} \subset \mathcal{J}^{2(\text{close})}$  is the set of train pairs that are planned to pass the same interlocking area of  $s$  in order to have  $j$  to departure  $s$  while  $j'$  arrive  $s$  from the direction of  $s'$ . Set  $(\forall s \in S \times S) \mathcal{J}_{s,s'}^{2(\text{switch,in,noMP})} \subset \mathcal{J}^{2(\text{close})}$  is the set of train pairs that are planned to pass the same interlocking area of  $s$  upon their arrival at  $s$  from the direction of  $s'$ , and there is no M-P possibility for them between  $s$  and  $s'$ . Set  $(\forall s \in S \times S) \mathcal{J}_{s,s'}^{2(\text{switch,in,MP})} \subset \mathcal{J}^{2(\text{close})}$  is the set of train pairs that are planned to pass the same interlocking area of  $s$  upon their arrival at  $s$  so that either they both come from the direction of  $s'$  but there is a M-P possibility for them between  $s$  and  $s'$ , or one of them is approaching  $s$  from a direction other than  $s'$ . Set  $(\forall j \in \mathcal{J}) \mathcal{C}_j^2$  is the set of all station pairs that are subsequent in the route of  $j$ . Set  $(\forall (j, j') \in \mathcal{J} \times \mathcal{J}) \mathcal{C}_{j,j'}^{2(\text{common})}$  is the set of all station pairs that appear as subsequent stations in the route of both  $j$  and  $j'$  heading in the same direction. Set  $(\forall (j, j') \in \mathcal{J} \times \mathcal{J}) \mathcal{C}_{j,j'}^{2(\text{common,single})}$  is the set of all station pairs that appear as subsequent stations in the route of both  $j$  and  $j'$  which are connected with a single-track line segment, and trains are heading in opposite directions. The order within the pairs is determined by  $j$ . All these sets can be enumerated based

on the input data in a straightforward manner.

## Parameters

The parameters that appear in our model are the following:

- $\tau^{(\text{pass})}(j, s \rightarrow s')$  is the running time of  $j$  from  $s$  to  $s'$ .
- $\tau^{(\text{headway})}(j, j', s \rightarrow s')$  is the minimal headway time for  $j'$  following  $j$  from  $s$  to  $s'$ .
- $\tau^{(\text{switch})}(j, j', s)$  is the running time of  $j$  over a interlocking area of  $s$ , where  $j$  may be in conflict with  $j'$ . (In our examples we do not consider cases when, e.g., on bigger stations there are multiple switches with different technological times. The model could trivially be extended to cover such scenarios by adding extra indices if relevant.)
- $\tau^{(\text{dwell})}(s, j)$  is the minimal dwell time of  $j$  at  $s$ .
- $\tau^{(\text{turn})}(s, j, j')$  is the minimum turnaround time for the rolling stock of a train  $j$  terminating at  $s$  to continue its journey as train  $j'$ .
- $\sigma(j, s)$  is the scheduled departure time of  $s$  from  $j$ , given by the original timetable.
- $v(j, s)$  is the earliest possible departure time of  $j$  from  $s$  when a disturbance in the network happens. It is the maximum of  $\sigma(j, s)$  and the technically feasible earliest departure time, and may be more constraining than the first depending on the initial delays. The latter is calculated assuming that the train follows its planned route at minimum running time and that there are no other trains present on the network.
- $d_{\max}$  is an upper bound assumed for the secondary delay  $t^{(\text{out})}(j, s) - v(j, s)$ . This parameter sets an upper limit for the possible secondary delays that can arise on a particular part of the network. Setting such a bound is common in the literature, see e.g. the work of [D'Ariano et al. \(2007\)](#). We set the same value of this parameter for all our testing instances. It has to be big enough so that no secondary delay exceeds it (e.g.  $d_{\max} = 40$  excludes the possibility of a one-hour delay due to waiting for another delayed train). Meanwhile, it is desirable to set its value as small as possible; restricting the time variables to small intervals decreases the number of binary decision variables in the model.

The choice of a small  $d_{\max}$  parameter results in a decrease of the model size, which is achieved via defining the set  $J^2(\text{close})$ . A pair of trains  $(j, j')$  is included in this set if and only if they can meet on any station, given the original timetable, the disturbed timetable, and assuming that no train can have a secondary delay greater than  $d_{\max}$ . The number of constraints will be proportional to the average number of trains that can meet another train at a station; this will be linear in  $d_{\max}$ .

## Decision variables

Our decision variables are the following. First, we use departure time variables:

$$t^{(\text{out})}(j, s) \in \mathbb{N} \quad (1)$$

defining the departure time of train  $j \in \mathcal{J}$  from station  $s \in \mathcal{S}_j$ . Such a variable is defined for all decision stations  $\mathcal{S}_j$ . In the case of trains that terminate within the modeled part of the network, the last station is not included in  $\mathcal{S}_j$ . The arrival time of the trains at stations,  $t^{(\text{in})}(j, s) \in \mathbb{N}$  are trivially related to the  $t^{(\text{out})}(j, s)$  variables through a constant offset (c.f. Eq. (3)), given the fixed running time assumption.

Second, in addition to the time variables, we use three sets of binary precedence variables. Decision variables  $y^{(\text{out})}(j, j', s) \in \{0, 1\}$  determine the order of trains to leave stations: the variable takes the value 1 if train  $j$  leaves station  $s$  before train  $j'$ , and 0 otherwise. The  $(j, j', s)$  tuples for which an  $y$  variable is defined will be specified later. Similarly, the precedence variables  $y^{(\text{in})}(j, j', s) \in \{0, 1\}$  prescribe the order at the entry to stations; the value is 1 if  $j$  arrives to  $s$  before  $j'$ . The last set of precedence variables describes the precedence of trains at some resource located between stations  $s$  and  $s'$  (e.g. a single-track segment used by  $j$  and  $j'$  heading in opposite direction). The binary variable  $z(j, j', s, s') \in \{0, 1\}$  will be 1 if  $j$  uses the given resource before  $j'$ . Also in this case, the quadruples  $(j, j', s, s')$  for which we have such a variable will be specified later.

## 4.2 ILP formulation

Given the index sets, variables, and the parameters and decision variables of the model, now we formulate the optimization objective and the constraints.

### Objective function

Our goal is to minimize the secondary delays that occur in the analyzed part of the railway network. Hence, a suitable objective function is the *weighted sum of secondary delays at the destination station*:

$$f(t) = \frac{1}{d_{\max}} \sum_{j \in \mathcal{J}} w(j) \left( t^{(\text{out})}(j, s^*) - v(j, s^*) \right). \quad (2)$$

where  $s^*$  is the last element of  $S_j$ , and  $w_j$  are weights for each train representing its priority. The reason for restricting ourselves to the secondary delays at the destination stations only is that this is the actual figure of merit chosen by the respective railway authorities; the generalization to other linear objectives such as the weighted sum of secondary delays on all stations is straightforward. The constant multiplier  $1/d_{\max}$  is optional; we use it for better comparability of different instances.

### Constraints

The constraints of the model are the following.

**Minimal running time** Each train needs a minimal time to get to the subsequent station:

$$\forall j \in \mathcal{J} \forall (s, s') \in \mathcal{C}_j \quad t^{(\text{in})}(j, s') = t^{(\text{out})}(j, s) + \tau^{(\text{pass})}(j, s \rightarrow s') \quad (3)$$

**Headways** A minimal headway time is required between subsequent train pairs on the common part of their route as

$$\begin{aligned} \forall (j, j') \in \mathcal{J}^2 \text{ (headway)} \quad \forall (s, s') \in \mathcal{C}_{j, j'}^2 \quad & t^{(\text{out})}(j', s) \geq \\ & t^{(\text{out})}(j, s) + \tau^{(\text{headway})}(j, j', s \rightarrow s') - C \cdot y^{(\text{out})}(j', j, s), \end{aligned} \quad (4)$$

where  $C$  is a constant big enough to make the constraint satisfied whenever the binary variable  $y^{(\text{out})}(j', j, s)$  takes the value of 1. (Constraints of this structure are often termed as big-M constraints in this context.) In our implementation, we calculate and use the smallest suitable value of  $C$  given particular  $d_{\max}$  value, i.e.

$$C = -\min(t^{(\text{out})}(j', s)) + \max(t^{(\text{out})}(j, s)) + \tau^{(\text{headway})}(j, j', s \rightarrow s') \quad (5)$$

**Single-track occupancy** Trains moving in opposite directions cannot meet on the same single-track line segment:

$$\begin{aligned} \forall (j, j') \in \mathcal{J}^2 \text{ (single)} \quad \forall (s, s') \in \mathcal{C}_{j, j'}^2 \quad & t^{(\text{out})}(j', s') \geq \\ & t^{(\text{in})}(j, s') - C \cdot z(j', j, s', s), \end{aligned} \quad (6)$$

where  $C$  is a big enough constant chosen similarly to that in Eq. (4).

**Minimal dwell time** Each train has to occupy the station node for a prescribed time duration at each station:

$$\forall j \in \mathcal{J} \forall s \in S_j \quad t^{(\text{out})}(j, s) \geq t^{(\text{in})}(j, s) + \tau^{(\text{dwell})}(j, s). \quad (7)$$

**Timetable** No train is allowed to depart before its scheduled departure time:

$$\forall j \in \mathcal{J} \forall s \in S_j \quad t^{(\text{out})}(j, s) \geq \sigma(j, s). \quad (8)$$

**Station track occupancy** Station tracks can be occupied by at most one train at a time:

$$\forall s \in S \forall (j, j') \in \mathcal{J}_s^2 \quad t^{(\text{in})}(j', s) \geq t^{(\text{out})}(j, s) - C \cdot y^{(\text{out})}(j', j, s), \quad (9)$$

where  $C$  is chosen similarly to that in Eq. (4) again. Note that this requirement may not be needed for depot tracks; the exceptions can be handled by the proper definition of  $\mathcal{J}_s^2$ .

**Interlocking area occupancy** These ensure that trains cannot meet in interlocking areas:

$$\begin{aligned} \forall s \in S \forall (j, j') \in \mathcal{J}_s^2 \text{ (switch,out)} t^{(\text{out})}(j', s) \geq \\ t^{(\text{out})}(j, s) + \tau^{(\text{switch})}(j, j', s) - C \cdot y^{(\text{out})}(j', j, s), \end{aligned} \quad (10)$$

$$\begin{aligned} \forall (s, s') \in S^{\times 2} \forall (j, j') \in \mathcal{J}_{s, s'}^2 \text{ (switch,out,in)} t^{(\text{in})}(j', s) \geq \\ t^{(\text{out})}(j, s) + \tau^{(\text{switch})}(j, j', s) - C \cdot z(j', j, s', s), \end{aligned} \quad (11)$$

$$\begin{aligned} \forall (s, s') \in S^{\times 2} \forall (j, j') \in \mathcal{J}_{s, s'}^2 \text{ (switch,in,noMP)} t^{(\text{in})}(j', s) \geq \\ t^{(\text{in})}(j, s) + \tau^{(\text{switch})}(j, j', s) - C \cdot y^{(\text{out})}(j', j, s'), \end{aligned} \quad (12)$$

$$\begin{aligned} \forall (s, s') \in S^{\times 2} \forall (j, j') \in \mathcal{J}_{s, s'}^2 \text{ (switch,in,MP)} t^{(\text{in})}(j', s) \geq \\ t^{(\text{in})}(j, s) + \tau^{(\text{switch})}(j, j', s) - C \cdot y^{(\text{in})}(j', j, s), \end{aligned} \quad (13)$$

with a choice of  $C$  similar again to that in Eq. (4).

**Rolling stock circulation constraints** These are introduced to bind the train with the shunting movement called also service train. If the train set of train  $j$  which terminates at  $s$  is supposed to continue its trip as (service train)  $j'$  or vice versa, a precedence of these trains including a minimum turnaround time has to be ensured:

$$\forall s \in S \forall (j, j') \in \mathcal{J}_s^2 t^{(\text{out})}(j', s) \geq t^{(\text{in})}(j, s) + \tau^{(\text{turn})}(j, j', s). \quad (14)$$

**Order of trains** We have additional conditions on the  $y$ -variables, concerning the case when M-O is not possible on the line or station.

$$\begin{aligned} \forall (j, j') \in \mathcal{J}^2 \text{ (headway)} \forall (s, s') \in \mathcal{C}_{j, j'}^2 \text{ (common)} \\ \forall (j, j') \in \mathcal{J}^2 \text{ (headway)} \cap \mathcal{J}_{s'}^2 \text{ (track)} \\ y^{(\text{out})}(j, j', s) = y^{(\text{out})}(j, j', s') \\ \forall (s, s') \in S^{\times 2} \forall (j, j') \in \mathcal{J}_{s, s'}^2 \text{ (switch,in,MP)} \cap \mathcal{J}_{s'}^2 \text{ (track)} \\ y^{(\text{in})}(j, j', s') = y^{(\text{out})}(j, j', s') \end{aligned} \quad (15)$$

The objective function in Eq. (2), together with the constraints in Eq. (3)-(14) define our mathematical programming model.

The model yields an integer linear program, and the time variables can be constrained even into a finite range using the parameter  $d_{\max}$ . Note that the binary variables have the obvious symmetry property

$$\begin{aligned} y^{(\text{out})}(j', j, s) &= 1 - y^{(\text{out})}(j, j', s) \\ z(j', j, s', s) &= 1 - z(j, j', s, s'), \end{aligned} \quad (16)$$

which is taken into account explicitly by using independent binary variables only.

As for the scaling of our model, the number of time variables i.e.  $\#t$  is bounded by number of trains times number of stations  $\#\mathcal{J}\#\mathcal{S}$  (see also Section 3.1 of the work of [Domino et al. \(2022b\)](#)). To obtain a more accurate estimate of the number of these variables we observe that in our model no trains visit all stations. We assume that in average each train visits  $\alpha \in (0, 1)$  fraction of the stations, we have then

$$\#(t) \approx \alpha \#\mathcal{J}\#\mathcal{S}. \quad (17)$$

as a tighter bound.

Suppose, that most of the network is composed mainly of double-track lines. Then there will be typically a single precedence variable per train and station ( $y^{(\text{out})}(j, j', s)$ ), and thus their number can be estimated by:

$$\#y + \#z \approx \#y \approx \alpha N(d_{\max}) \#\mathcal{J}\#\mathcal{S}, \quad (18)$$

where  $N(d_{\max})$  is the number of trains the train can meet at a station on average. Under such assumptions, the total number of variables grows linearly with number of trains and stations:

$$\#vars = \#t + \#y + \#z \approx \text{const} \#\mathcal{J}\#\mathcal{S}. \quad (19)$$

If, on the other hand, the network has dominantly single-track lines, two precedence variables per train and station ( $y^{(out)}(j, j', s)$  and  $z(j, j', s, s')$ ) will be needed, and thus

$$\#y = \#z \approx \alpha N(d_{\max}) \#\mathcal{J} \#\mathcal{S}. \quad (20)$$

In both cases we assume that there are not many ( $y^{(in)}(j, j', s)$ ) variables, as they are tied certain particular interlocking area conditions.

Based on Eq. (16) there are typically 2 constraints per each  $y$  variable as headway and station track occupation constraints, and 2 constraints per each  $z$  variable as single-track occupation constraints. For the interlocking area occupation constraints, it is more complicated as it involves both  $z$  and  $y$  variables; a good assumption is to consider 2 constraints for each  $y$  variable. For the running time and minimal dwell time we expect one constraint per train and station. This number of constraints can be estimated by

$$\#constr. \approx 6\#y + 2\#z + 2\#\mathcal{J} \#\mathcal{S} \quad (21)$$

where the second term is tied to single-track line conditions (one condition per  $z$  variable).

$$\#constr. \approx \begin{cases} \alpha(6N(d_{\max}) + 2)\#\mathcal{J} \#\mathcal{S} & \text{for double-track} \\ \alpha(8N(d_{\max}) + 2)\#\mathcal{J} \#\mathcal{S} & \text{for single-track.} \end{cases} \quad (22)$$

Because of the limitations in time imposed by  $d_{\max}$  the model can be viewed as linear in number of trains and number of stations. Hence, as expected, the model is more complex for the network in which single-track lines dominate. Although the analyzed network is mostly composed of the double-track lines, we will analyze certain use-cases with the fraction of single-track lines increased.

Observe that without limiting the secondary delays by  $d_{\max}$ , the value of  $N(d_{\max})$  would only be bounded by  $\#\mathcal{J} - 1$  (as each train is considered to possibly meet each other), which would result in quadratic scaling of the number of precedence variables, and that of the number of constraints in the number of trains.

## 5 Hybrid quantum-based approach

To overcome the limitations described in Section 2 of current hardware quantum annealers, we apply a hybrid (quantum-classical) solver. In particular, we use the 'Leap Hybrid Solver Service (HSS)' (D-Wave Quantum Inc., 2022a); a cloud-based proprietary solver that is developed by the market leader of QA hardware and is available as a service. It utilizes a hybrid approach that combines classical computational power with quantum processing.

In particular, we have used the Constrained Quadratic Model (CQM) (D-Wave Quantum Inc., 2022b) Solver. The CQM hybrid solver works as follows.

**Input** A constrained linear or quadratic model, and the value of the solver parameter  $t_{\min}$ , which prescribes the minimum required run time (in seconds) the solver is allowed to work on any problem.

**Preprocessing** Preprocessing includes subproblem identification and decomposition to smaller instances (Tran et al., 2016). Furthermore, the solver's internal preprocessing mechanism takes constraints into account automatically, implementing the suitable penalty method internally.

**Processing** The hybrid solver implements a workflow that combines a portfolio of various classical heuristics (including tabu search, simulated annealing, etc.) running on powerful CPUs (Central Processing Units) and GPUs (Graphics Processing Units). In the course of the solution process the hardware quantum annealer is also invoked, to solve smaller QUBO problems that can potentially boost the classical heuristics. Integer problems are transformed to binary using state-of-the-art methods like the one described by Glover et al. (2019); Karimi and Ronagh (2019), generally applicable for integer problems. When using the quantum hardware, the solver performs the required embedding, runs the QUBO subproblem on the physical QA device several times, and returns a sample of potential solutions. After these readouts, the sample is incorporated into the solution workflow. In this way, even though the physical annealer supports problems with limited size (e.g. the Pegasus machine has 5500 physical qubits (Dattani et al., 2019), and several of these may be needed to represent a binary variable because of the embedding), the approximate solutions of small subproblems contribute to the solution process. The final solution is composed by the solver's module.

**Output** The solution or solutions of quadratic constrained problem or the integer problem. The workflow results in a solution or solutions that are not guaranteed to be optimal, hence, the hybrid solver as a whole is in nature a heuristic solver. Furthermore, the solver is probabilistic, hence at each run the final output can be different. The CQM (integer) solver returns a series of solutions, which can be an additional asset. Nevertheless, for sake of presentation, our approach is to analyze only the best CQM solution given each run of the hybrid algorithm (realization).

While D-Wave's proprietary solvers act as black boxes, i.e. they hide the exact details of the described process from the user, the output is supplemented with timing parameters, including *run time*: the total elapsed time including system overhead, and *Quantum Processing Unit (QPU) access time* which is the time spent accessing the actual quantum hardware. These parameters enable a comparison with other solvers.

As mentioned before, in addition to the actual problem to be solved, the CQM solver optionally inputs another parameter,  $t_{min}$ . This is a time limit for heuristics running in parallel (D-Wave Quantum Inc., 2022b): unless a thread does not terminate by itself after  $t_{min}$ , it is allowed to run at least till  $t_{min}$  before it is stopped at the current best solution. We have sampled the CQM problems with various settings of  $t_{min}$  and uncovered the impact of this setting on the model performance and solution quality for our problem.

The CQM Solver can solve problems encoded in the form of Eq. (2) – (15) (c.f. Section 4.2) with up to 5000 binary or integer variables and 100,000 constraints. Computational results of railway rescheduling problems were obtained using classical as well as hybrid (quantum-classical) solvers. As a classical solver, IBM ILOG CPLEX Interactive Optimizer (version 22.1.0.0) was used. The CPLEX computation was performed on 16 cores of *Intel(R) Core(TM) i7-10700kF CPU 3.80GHz* with 64GBs of memory. As a hybrid solver, the D-Wave CQM hybrid solver (version: 1.12) was used.

## 6 Computational results

In this section, we demonstrate the performance of the proposed hybrid (quantum-classical) approach on a network at Polish railways - the central part of the Upper Silesia Metropolis. In particular, we compare the performance of D-Wave's hybrid quantum-classical solver (CQM) with CPLEX. The comparison is performed for diverse network layouts including single-, double-, and multiple-track lines, and different level of disturbances including various initial delays and track closures. As the objective is tied to secondary delays, we can roughly apply it to assess the degree of difficulty of the problem.

Section 6.1 describes the considered network and traffic characteristics. Section 6.2 presents results concerning generic examples on the core line of the network, comparing double-track-line scenarios with single-track-line scenarios and closure scenarios. Section 6.3 presents analogous results for larger network with real-life timetable. Here the case studies concern various scenarios with different degrees of difficulty.

### 6.1 Railway network

We use the Open Railway Map<sup>1</sup> representation of the selected part of the Polish railway network located in the central part of the Metropolis GZM (Poland), presented in Fig 2. The selected part of the network combines a heterogeneous network layout including single-, double-, triple-, and quadruple-track lines. It comprises 25 nodes including 11 stations and 3 junctions, 146 blocks, and 2 depots. The infrastructure is managed by Polish state infrastructure manager PKP PLK (Polskie Koleje Państwowe, Polskie Linie Kolejowe eng. Polish State Railways, Polish Railway Lines).

The decision stations include stations  $\{KO, KO(STM), CB, KL\}$ , stations bounding the analyzed part of the network  $\{GLC, CM, KZ, Ty, Mi\}$ , depots  $\{KO(KS), KO(IC)\}$  from which regional and intercity trains are being shunted to and from  $\{KO\}$ , and stations on the single-track line –  $\{MJ\}$  to allow meet and pass (M-P) or meet and overtake (M-O). As described before, the decision stations are the only ones that appear explicitly in our model. Due to operational reasons resulting from track design, the decisions on train departure times (and thus on trains' order) are, in the current operational practice, *de facto* made with respect to the decision stations. All other stations and junctions are treated as line blocks as long as no rerouting or retracking is considered; they will appear in the model implicitly via parameters. These stations include:

---

<sup>1</sup><https://www.openrailwaymap.org/>, visited 2022-11-25

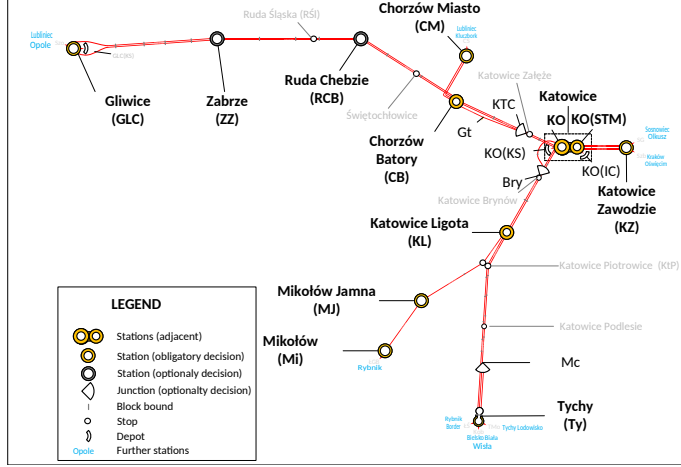


Figure 2: Selected part of Polish railway network located in the central part of the Metropolis and examined in our research.

- stations  $\{ZZ, CB\}$  in which usually there are rigid assignments of the platform tracks to the traffic direction (i.e., track 1 towards  $\{GLC\}$ ; track 2 towards  $\{KO\}$ )
- branch junctions  $\{KTC, Bry, Mc\}$  in which usually there is a rigid assignment to the tracks.

As an example, let for a particular train  $j$ ,  $\hat{\mathcal{S}}_j = \{KZ, KO(STM), KO, KTC, CB, RCB, ZZ, GLC\}$  be the ordered set of stations. Then, the dispatching decisions *de facto* affect directly the *decision stations*  $\mathcal{S}_j = \{KZ, KO(STM), KO, CB, GLC\}$ . The set of decision stations can be extended if necessary.

In all computation priority weights in Eq. (2) we use  $w_j = 1$  for stopping (local) trains  $w_j = 1.5$  for intercity (fast) trains  $w_j = 1.75$  for express trains, and  $w_j = 0$  for shunting (if applicable). As for the solver parameter  $t_{\min}$ , after initial experiments, we have decided to prefer  $t_{\min} = 5$  s as it provides a good balance between computation time and expected solution quality. A sensitivity analysis regarding this parameter will be performed in Section 6.3.

## 6.2 Synthetic experiments on the selected railway line

As the first set of experiments we address, synthetic instances on a part of the network - railway line KO-GLC, see Fig 2. The goal in these scenarios is to compare the CPLEX and CQM solvers for: the double-track line (*line1*), the double-track line with closures (*line2*), and the single-track line (*line3*). Shunting movements and rolling stock circulation are not considered in this set of experiments. In particular, the addressed configurations are the following:

1. *Line1*, the double-track line with dense traffic. We use cyclic 3-hour timetable with 10 trains each hour and each direction, i.e. we have 59 trains.
2. *Line2*, similar to *line1*, with the additional closure of one of the tracks between ZZ and RCB. We use a cyclic 2-hour timetable with 10 trains each hour and each direction, i.e. we have 40 trains.
3. *Line3*, the whole line is considered as a single-track, with a timetable of 3 hours traffic and 21 trains.

For *line1* and *line3*, the original timetable is feasible, while for *line2* it is not feasible due to the closure. For each of the lines, we compute 12 instances, each with different initial delays of train subsets. Instance 0 yields no initial delays. Thereafter, we use the parameter value  $d_{\max} = 40$  min, in all cases in this and subsequent subsection. Assuming that each train interacts with  $N(d_{\max}) = 12$  trains for *line1* and *line2*, and with  $N(d_{\max}) = 6$  trains for *line3*, Eqs. (17) - (19), (22) allows us to quickly estimate the sizes of the problem. These sizes are compared with the computed (comp.) actual number of variables and constraints (mean over instances) in Tab. 1. Here, *line2* is the most complex in terms of constraints, which is reflected later by the computational difficulties of some of its instances. Furthermore, *line2* is partially double-track and partially single-track, hence the actual number of constraints is bounded from above by the estimate

1	# $\mathcal{S}$	# $\mathcal{J}$	# int vars		# precedence vars		# constraints	
			comp. mean	Eq. (17)	act. mean	Eq. (18)/Eq. (20) doub./sing.	comp. mean	Eq. (22) doub./sing.
1	3	59	118	118	1538	1415 / -	7889	8731 / -
2	5	40	142	133	1394	1600/3200	8491	6867/13067
3	5	21	79	70	592	- / 840	3057	- / 3499

Table 1: Synthetic experiments. The first column is the ordinal number of the line. For the estimated and actual number of variables and constraints, we use  $\alpha = 2/3$  in Eqs. (17) - (19), (22) (doub. - double-track, sing. - single-track, comp. mean - computed actual number of variables or constraints, mean over instances).

for the single-track line and from below by the estimate for the double-track line. *Line1* includes double-, whereas *line3* single-track segments only. There actual number of constraints and variables appeared to be close to the estimate.

The computational results are presented in Fig. 3 a) b) c) for *line1*, *line2*, and *line3*, respectively. Each figure shows objective  $\times d_{\max}$  (top part), computation time (comp. time, middle part), and QPU access time (bottom part) for CQM hybrid solver with  $t_{\min}$  equal 5 and 20s. CPLEX results are also displayed.

For scenario *line1* (Fig. 3 a) ), the CQM solver obtained optimal solutions for all cases (except for instances 6 and 11). Similarly, for *line3* (Fig. 3 c) ), only small deviations from the optimum can be observed for a number of instances. All computational times for *line1* and *line3* were significantly below 0.4min, although CPLEX performed faster. Comparing CQM with  $t_{\min} = 5s$  and  $t_{\min} = 20s$ , we have almost the same objectives but  $t_{\min} = 20s$  requires almost 4 times longer computational time.

For *line2* (Fig. 3 b) ), all CQM solutions were suboptimal, although feasible. More remarkably, for 9 instances at  $t_{\min} = 5s$  and 3 instances at  $t_{\min} = 20s$  (out of 12 instances) CQM was faster than CPLEX, in several cases up to 5× faster. This difference in time is clear while setting the minimal processing time of the CQM solver  $t_{\min} = 5s$  (see Section 5). In principle, *line1* (Fig. 3 a) ) and *line3* (Fig. 3 c) ) are less complicated in terms of number of constraints, and here solutions of CPLEX and CQM are similar in terms of objective, but CPLEX is faster. We can conclude that the utility of the CQM solver can be expected for the more complex instances of railway scheduling problems.

### 6.3 Real-life experiments on the considered rail network

In this subsection, we will test the CQM solver on more realistic scenarios of the railway traffic on the presented network. We will also focus on the track closure situation, turning a double-track line segment into a single-track one, under dense traffic, to elaborate our findings from *line2* in Section 6.2. Our computations address various use cases of train delays outside the network and within the network as well as the partial track closure. We constructed 9 networks with increased levels of difficulty ranging from small delays to disruptions, i.e. it is expected more trains are involved and/or disturbances are spread more over the network. These networks are tabulated in Table 2. Their details are as follows:

1. Networks 1 - 3 concern only disturbances due to delayed trains and no closures.
2. Networks with number 4 or higher concern also disturbances due to closures.
  - (a) Networks 4 and 5 concerns rerouting trains from double-track line KTC-CB to the single-track line with higher passing times, see Fig. 2 (trains have no initial delays in network 3 and some initial delays in network 4).
  - (b) Network 6 concerns multiple closures, i.e. change of multiple line KZ-KO(STM) and double-track line KO-KL to single-track lines. (See Fig. 2; the reason can be e.g. upcoming reconstruction works on this part of network.)
  - (c) Networks 7 - 9 concerns closures of both 5 and 6, but each with different initial delays of trains. The intention of the last 3 networks is to create a really challenging rescheduling problem.
3. For comparison, network 0 is the default problem with no disturbances.

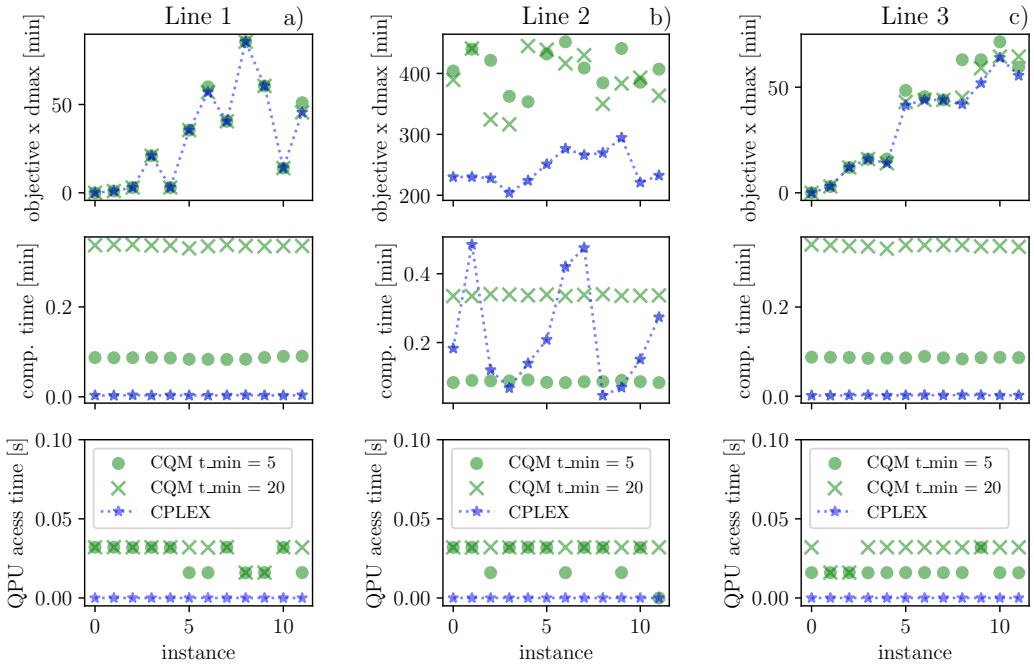


Figure 3: Synthetic experiments *Line1*, *Line2*, *Line3* comparison of the performance of classical solver (CPLEX) with that of the hybrid CQM. All the displayed solutions are feasible. Total computational time (middle panel) and QPU times (lower panel) were provided by the D-Wave output. Panel a) - *line1*, results of both solvers were similar in terms of the objective, but the CPLEX computation was faster. Panel b) - *line2* namely the double-track line with closures and dense traffic, has appeared to be most challenging for both the classical solvers (in terms of computational time) and for the quantum solver (in terms of objective). On this example, there are instances, where the current CQM D-Wave hybrid solver outperforms CPLEX in terms of computational time. Increasing the value of the  $t_{\min}$  parameter in most cases improves the quality of the solution at the cost of computational time. Panel c) - *line3* all the displayed solutions are feasible. Results of both solvers were similar in terms of the objective, but CPLEX computation was faster.

Table 3 tabulates the results comparing CPLEX and CQM in terms of objective function value and computation time; problem sizes and QPU times are included. As CQM is probabilistic, 5 runs have been performed for each network, yielding 5 different realizations. This also facilitates the analysis of the statistics of the output and the differences between particular realizations.

The level of difficulty increases with the number of variables and constraints. Observe that CQM always returns a feasible solution. For the networks 0–3 with initial delays only, CQM generated optimal solutions, while in the remaining networks, the objective value was somewhat higher than the actual optima obtained with CPLEX. As for computational times, for CPLEX they grow significantly - from 0.072 to almost 8s (network 9). Meanwhile, those of CQM remain almost constant around 5.1s. QPU times remain not greater than 0.032s. Remarkably, for the hardest instances: networks 7 and 9, the CQM hybrid solver even outperforms CPLEX with respect to computational time. It does not find the actual optimum, just a feasible solution close to it. For example, in network 9, the computed CQM solution is around 30% worse than the optimal one. In conclusion, we expect benefits from the application of the hybrid solver on medium-scale railway networks with multiple closures, as in networks 7–9. This finding follows our observation on synthetic data in Fig. 3 b), where the benefits appeared for more complex instances, too.

To evaluate the extent of difficulty of the problems analyzed in Tab. 3, Tab. 4 presents mean (over stations and realizations) delays, resulting from CQM solutions, on selected stations (i.e. stations in the central part of the network in Fig. 2). Meaningful delays are introduced starting from network 4 onward, i.e. for networks with closures in a limited number of stations, see also Tab. 2. From network 5 onward, delays become more uniformly distributed among the stations when compared with results in Tab. 2. However, for networks 7–9 the mean delays are the highest and almost uniformly distributed among all stations, showing

network	#S	place	trains involved	description
<b>A. Disturbances from outside the network</b>				
1	10	KO-Ty	IC 14006 KS 94113	Delayed IC (higher priority) is in conflict with on-time KS
2	10	arr. Ty	KS 94766 KS 40518 IC 41004 KS 44862 IC 4120	Delayed 5 trains on the arrival to Ty, random delays of several minutes
<b>B. Disturbances originated within the network</b>				
3	10	whole network	14 trains KS + IC	Random delays of 14 trains delays up to 35 minutes
<b>C. Disturbances within the network and closures</b>				
4	11	KTC-CB	10 trains KS + IC	double-track line KTC-CB closed trains rerouted to single-track line
5	11	whole network	most trains	double-track line KTC-CB closed as in 4 + delays as in 3
6	10	whole network	all trains	multiple-track KZ - KO(STM) and double-track KO - KL changed into single-track + delays as in 3
7	11	whole network	all trains	multiple-track KZ - KO(STM) and double-track KO - KL changed into single-track + double-track line KTC-CB closed as in 4 + delays as in 3
8	11	whole network	all trains	Closures as in 7 + random delays of 13 trains up to 30 minutes
9	11	whole network	all trains	Closures as in 7 + random delays of 15 trains up to 30 minutes

Table 2: Real-life experiments. Networks of particular dispatching problems. In networks 0 - 5 most of analyzed network is double-tracked, from network 6 upward the number of single-track lines in the network increases at the expense of the number of double and multiple-track lines. For each network we considered a two-hour time with an afternoon rush-hour timetable from the year 2021, with  $\#J = 27$  trains. Beside the  $\#S$  stations there are 2 depots in each network.

that the spread of disruption impacts the whole network. These have appeared to be more challenging network disruptions.

Fig. 4 shows a more detailed statistical analysis for two networks 4 and 7 and compares CPLEX (left, red) vs CQM (right, blue). For network 4, bigger delays occur mainly at stations KO(STM), KO and CB for both CPLEX and CQM solutions, albeit for the former are somewhat smaller. This reflects the initial disturbances, which indeed occurred mainly between KO and CB (see Tab. 2), and thus the spread is limited to these 3 stations. For network 7, delays are more spread through the network due to disruption and initial disturbances. To conclude, we can expect an advantage from a hybrid (quantum-classical) approach, particularly in case of more complex problems with extensive disruptions and disturbances occurring throughout the whole network. To facilitate further evaluation of the solutions, train diagrams are presented in Appendix A.

The right choice of the  $\tau_{\min}$  parameter can improve results meaningfully. Let us analyze in more detail the role of the  $\tau_{\min}$  solver parameter for selected problems. In particular, for networks 7 and 9 therein, we have performed runs with  $\tau_{\min}$  sweeping over a range [5, 60]; the results are presented in Fig. 5 a) and b). The objective value is roughly log-linear in computational time. For small  $\tau_{\min}$  parameter values the computational time is shorter, whereas for large  $\tau_{\min}$  it grows exponentially. Overall, the improvement in the objective is overwhelmed by the increase of computational time. This is important from the point of view of the algorithm layout, as it may be tied to a power law scaling. Such behavior is plausible in the case of QA methods (Soriani et al., 2022; Albash et al., 2017; Domino et al., 2022a).

n.	CPLEX			CQM hyb. $t_{\min} = 5$ s mean value over 5 realiz.			comparison CQM vs. CPLEX	
	#vars / # constr.	obj. $\times$ dmax	comp. time [s]	obj. $\times$ dmax	comp. time [s]	QPU time [s]	obj. diff. %	comp t. diff %
0	556 / 1756	0.0	0.07	0.0	5.19	0.03	0 %	-
1	556 / 1756	1.0	0.08	1.0	5.24	0.02	0 %	-
2	556 / 1740	6.0	0.08	6.0	5.37	0.03	0 %	-
3	556 / 1769	7.5	0.09	7.5	5.05	0.03	0 %	-
4	662 / 2210	78.25	0.20	82.70	5.10	0.03	-5.6 %	-
5	662 / 2204	114.75	0.25	132.55	5.25	0.02	-15.5 %	-
6	711 / 2599	91.25	0.41	142.3	5.14	0.03	-55.9 %	-
7	817 / 3029	188.75	7.98	263.4	5.12	0.02	-39.5 %	35.8 %
8	817 / 3074	157.75	3.70	271.65	5.12	0.02	-72.2 %	-38.4 %
9	817 / 3081	185.5	6.51	263.85	5.11	0.02	-42.2 %	21.5 %

Table 3: Real-life experiments. Results of ILP optimization on CPLEX and CQM D-Wave hybrid solver.  $d_{\max} = 40$  was set for all networks. Computational times and QPU time were reported in D-Wave’s output. We have selected  $t_{\min} = 5$  s as it provides the best balance between computational time and the quality of solution. The last columns present a percentage comparison (CQM - CPLEX) / CPLEX, hence, the positive values represent CQM advantage, whereas negative values show CPLEX advantage.

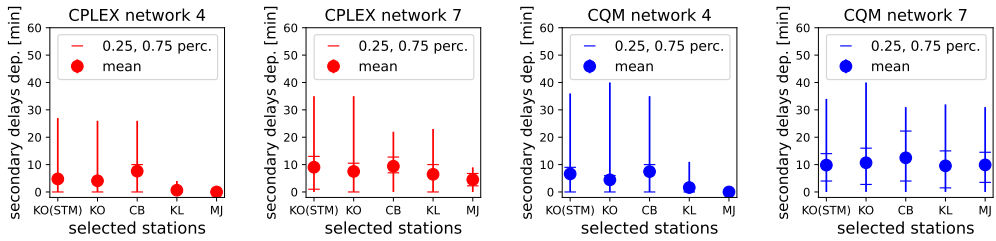


Figure 4: Real-life experiments. Statistics of CPLEX (left, red) and CQM (right, blue) solutions (Tab. 3) for selected networks in Tab. 2. The statistics were calculated over trains in the classical cases, and over trains and realizations in the CQM cases. Vertical lines are ranges, while horizontal lines are 0.25 and 0.75 percentiles.

## 7 Conclusions

We have demonstrated that quantum annealers can be readily applicable in train rescheduling optimization in urban railway networks. In particular, we have encoded rescheduling problems in a linear integer program and solved these using a state-of-the-art solver (CPLEX), as well as the QA based CQM hybrid (quantum-classical) solver. The results suggest that quantum computing and QA in particular, although an early-stage technology, are ready to tackle challenging railway rescheduling problems. While the CQM hybrid solver does not outperform classical solvers in general, we have found specific cases in which they were actually better. This supports the expectation that future quantum devices will be efficient in solving large-scale problems, and in our case, real-time railway dispatching problems on the national scale; even in the range that is beyond the scope of current exact models and heuristics.

While the quantum-based solvers possibly return suboptimal solutions, these are still feasible and often better than the solutions obtained manually or based on smaller-scale models. In each computation, the CQM hybrid solver always has taken some advantage of the QPU. Hence, such a little help from the QPU must have boosted the classical heuristics in the hybrid solver, even if quantum annealer devices are subjects of many ongoing debates.

Several future research directions can be determined. The first concerns the ongoing worldwide works on the development of fault-tolerant quantum computing devices (DiVincenzo, 2000) with proper error correction/mitigation, this will boost results of approaches supported by quantum computing (and QA in particular). The second concerns the creation of a custom open-source hybrid solver that is dedicated

network	Delay [min]				
	KO(STM)	KO	CB	KL	MJ
0	3.7	1.0	1.7	1.5	0.0
1	3.1	1.3	2.1	1.5	0.0
2	3.8	1.3	2.0	1.3	2.0
3	2.6	2.1	1.4	0.7	1.5
4	6.6	4.4	7.4	1.6	0.0
5	7.1	6.2	10.7	1.0	2.7
6	6.7	6.7	3.2	8.7	4.1
7	9.8	10.7	12.5	9.5	9.9
8	10.4	10.5	10.0	10.5	7.6
9	10.0	10.3	11.5	9.8	9.6

Table 4: Real-life experiments. Mean (over trains and realizations) secondary delay resulted from CQM solutions (Tab. 3) for all networks in Tab. 2. Non-zero values for network 0 come from counted delays in shunting movement in KO and KO(STM) that are not included in the objective, as well as some cases where the train gets a few minutes, delay but makes it up and leaves the network on time - these are typical issues for the railway traffic on analyzed network.

to railway problems and will use the noise of quantum device to our advantage e.g. by modeling some stochastic behavior on railways. The third concerns the evolution and application of quantum-inspired techniques such as tensor networks technique, and simulated bifurcation (Goto, 2019). With all these future developments, QA-based approaches tend to become more powerful and ready to address for the first time large-scale real-time challenges in railway traffic management, which are currently unsolvable with traditional techniques.

## Data availability

The code and the data used for generating the numerical results can be found in [https://github.com/iitis/railways\\_dispatching\\_silesia](https://github.com/iitis/railways_dispatching_silesia) under DOI 10.5281/zenodo.10657323

## Acknowledgments

This research was supported by the Ministry of Culture and Innovation and the National Research, Development and Innovation Office within the Quantum Information National Laboratory of Hungary (Grant No. 2022-2.1.1-NL-2022-00004) (MK), and by the Silesian University of Technology Rector's Grant no. BKM - 720/RT2/2023 12/020/BKM\_2023/0252 (KK). This research was funded in part by National Science Center, Poland, under grant number 2019/33/B/ST6/0201 (LB) and 2023/07/X/ST6/00396 (KD). For the purpose of Open Access, the authors has applied a CC-BY public copyright license to any Author Accepted Manuscript (AAM) version arising from this submission.

We would like to thank Sebastian Deffner as well as the whole scientific community of the Department of Physics, University of Maryland, Baltimore County (UMBC) for valuable discussion; and to Bartłomiej Gardas, and Zbigniew Puchała for valuable motivation; and Katarzyna Gawlak, Akash Kundu, and Özlem Salehi for data validation and assistance with coding. We acknowledge the cooperation with Koleje Śląskie sp. z o.o. (eng. Silesian Railways).

## References

Albash, T., Martin-Mayor, V., and Hen, I. (2017). Temperature scaling law for quantum annealing optimizers. *Physical Review Letters*, 119(11):110502.

Avron, J. E. and Elgart, A. (1999). Adiabatic theorem without a gap condition. *Commun. Math. Phys.*, 203(2):445–463.

Bian, Z., Chudak, F., Macready, W. G., and Rose, G. (2010). The Ising model: teaching an old problem new tricks. visited 2022.04.29.

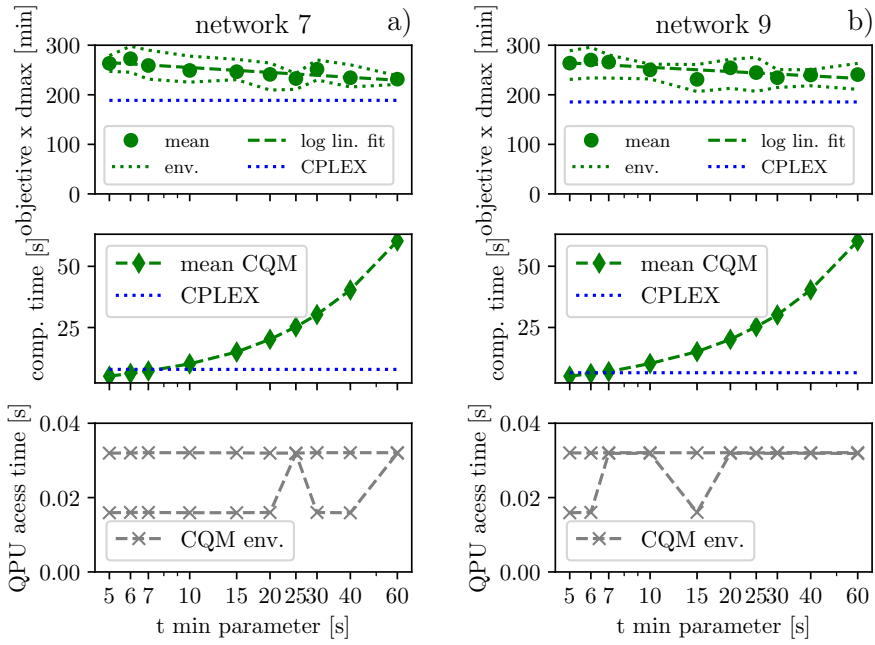


Figure 5: Real-life experiments. The sweep over  $t_{\min}$  parameter for network 7 a) and network 9 b), see Tab. 2. All solutions were feasible. For higher  $t_{\min}$  we expect smaller objective values but higher total computational time. For each parameter value, there were 5 realizations of the experiment were performed. Interestingly, a linear (negatively sloped) relation between the objective and the logarithm of  $t_{\min}$  can be observed, suggesting power law scaling.

Bickert, P., Grozea, C., Hans, R., Koch, M., Riehn, C., and Wolf, A. (2021). Optimising rolling stock planning including maintenance with constraint programming and quantum annealing. *arXiv preprint arXiv:2109.07212v1*.

Cacchiani, V., Huisman, D., Kidd, M., Kroon, L., Toth, P., Veelenturf, L., and Wagenaar, J. (2014). An overview of recovery models and algorithms for real-time railway rescheduling. *Transportation Research Part B: Methodological*, 63:15–37.

Caimi, G., Fuchsberger, M., Laumanns, M., and Lüthi, M. (2012). A model predictive control approach for discrete-time rescheduling in complex central railway station areas. *Computers & Operations Research*, 39(11):2578–2593.

Corman, F., D’Ariano, A., Pacciarelli, D., and Pranzo, M. (2012). Bi-objective conflict detection and resolution in railway traffic management. *Transportation Research Part C: Emerging Technologies*, 20(1):79–94. Special issue on Optimization in Public Transport+ISTT2011.

D-Wave Quantum Inc. (2022a). D-Wave Hybrid Solver Service: An Overview [WhitePaper]. visited 2022.04.29.

D-Wave Quantum Inc. (2022b). Hybrid Solver for Constrained Quadratic Model [WhitePaper]. visited 2022.04.29.

D’Ariano, A., Pacciarelli, D., and Pranzo, M. (2007). A branch and bound algorithm for scheduling trains in a railway network. *European Journal of Operational Research*, 183(2):643–657.

Das, A. and Chakrabarti, B. K. (2008). *Colloquium* : Quantum annealing and analog quantum computation. *Reviews of Modern Physics*, 80(3):1061–1081.

Dattani, N., Szalay, S., and Chancellor, N. (2019). Pegasus: The second connectivity graph for large-scale quantum annealing hardware. *arXiv preprint arXiv:1901.07636*.

DiVincenzo, D. P. (2000). The physical implementation of quantum computation. *Fortschritte der Physik: Progress of Physics*, 48(9-11):771–783.

Domino, K., Koniorczyk, M., Krawiec, K., Jałowiecki, K., Deffner, S., and Gardas, B. (2023). Quantum annealing in the NISQ era: railway conflict management. *Entropy*, 25(2):191.

Domino, K., Koniorczyk, M., and Puchała, Z. (2022a). Statistical quality assessment of ising-based annealer outputs. *Quantum Information Processing*, 21(8):288.

Domino, K., Kundu, A., Salehi, Ö., and Krawiec, K. (2022b). Quadratic and higher-order unconstrained binary optimization of railway rescheduling for quantum computing. *Quantum Information Processing*, 21(9):1–33.

Ge, L., Voß, S., and Xie, L. (2022). Robustness and disturbances in public transport. *Public Transport*, 14:191–261.

Glover, F., Kochenberger, G., and Du, Y. (2019). Quantum bridge analytics i: a tutorial on formulating and using qubo models. *4or*, 17:335–371.

Goto, H. (2019). Quantum computation based on quantum adiabatic bifurcations of Kerr-nonlinear parametric oscillators. *Journal of the Physical Society of Japan*, 88(6):061015.

Gusmeroli, N., Hrga, T., Lužar, B., Povh, J., Siebenhofer, M., and Wiegele, A. (2022). BiqBin: A parallel branch-and-bound solver for binary quadratic problems with linear constraints. *ACM Trans. Math. Softw.*, 48(2):1–31.

Harrod, S. (2011). Modeling network transition constraints with hypergraphs. *Transportation Science*, 45(1):81–97.

Ising, E. (1925). Beitrag zur theorie des ferromagnetismus. *Z. Physik*, 31(1):253–258.

Karimi, S. and Ronagh, P. (2019). Practical integer-to-binary mapping for quantum annealers. *Quantum Information Processing*, 18(4):1–24.

Kurowski, K., Węglarz, J., Subocz, M., Różycki, R., and Waligóra, G. (2020). Hybrid quantum annealing heuristic method for solving job shop scheduling problem. In Krzhizhanovskaya, V. V., Závodszky, G., Lees, M. H., Dongarra, J. J., Sloot, P. M. A., Brissos, S., and Teixeira, J., editors, *Computational Science – ICCS 2020*, pages 502–515, Cham. Springer International Publishing.

Lamorgese, L., Mannino, C., Pacciarelli, D., and Krasemann, J. T. (2018). Train dispatching. In Borndörfer, R., Klug, T., Lamorgese, L., Mannino, C., Reuther, M., and Schlechte, T., editors, *Handbook of Optimization in the Railway Industry*, pages 265–283. Springer International Publishing, Cham.

Lange, J. and Werner, F. (2018). Approaches to modeling train scheduling problems as job-shop problems with blocking constraints. *Journal of Scheduling*, 21(2):191–207.

Lusby, R. M., Larsen, J., Ehrhart, M., and Ryan, D. M. (2013). A set packing inspired method for real-time junction train routing. *Computers & Operations Research*, 40(3):713–724.

Mascis, A. and Pacciarelli, D. (2002). Job-shop scheduling with blocking and no-wait constraints. *European Journal of Operational Research*, 143(3):498–517.

Meng, L. and Zhou, X. (2014). Simultaneous train rerouting and rescheduling on an n-track network: A model reformulation with network-based cumulative flow variables. *Transportation Research Part B: Methodological*, 67:208–234.

Philip, E. M. and Swapnesh, S. (2022). A review on quantitative models and algorithms for real-time railway rescheduling. In *2022 Second International Conference on Next Generation Intelligent Systems (ICNGIS)*, pages 1–5.

Punnen, A. P., editor (2022). *The Quadratic Unconstrained Binary Optimization Problem: Theory, Algorithms, and Applications*. Springer International Publishing.

Soriani, A., Nazé, P., Bonança, M. V., Gardas, B., and Deffner, S. (2022). Three phases of quantum annealing: Fast, slow, and very slow. *Physical Review A*, 105(4):042423.

Szpigel, B. (1973). Optimal train scheduling on a single line railway. *Operational Research*, 72:343–352.

Törnquist, J. (2007). Railway traffic disturbance management—An experimental analysis of disturbance complexity, management objectives and limitations in planning horizon. *Transportation Research Part A: Policy and Practice*, 41(3):249–266.

Tran, T., Do, M., Rieffel, E., Frank, J., Wang, Z., O’Gorman, B., Venturelli, D., and Beck, J. (2016). A hybrid quantum-classical approach to solving scheduling problems. In *Proceedings of the International Symposium on Combinatorial Search*, volume 7, pages 98–106. AAAI Press, Washington, DC, USA.

Venturelli, D., Marchand, D. J., and Rojo, G. (2015). Quantum annealing implementation of job-shop scheduling. *arXiv preprint arXiv:1506.08479*.

Xu, H.-Z., Chen, J.-H., Zhang, X.-C., Lu, T.-E., Gao, T.-Z., Wen, K., and Ma, Y. (2023). High-speed train timetable optimization based on space–time network model and quantum simulator. *Quantum Information Processing*, 22(11):418.

Zbinden, S., Bärtschi, A., Djidjev, H., and Eidenbenz, S. (2020). Embedding Algorithms for Quantum Annealers with Chimera and Pegasus Connection Topologies. In *International Conference on High Performance Computing*, pages 187–206. Springer.

## Appendix A. Train diagrams of CPLEX and CQM

To further evaluate the solutions, we present time-distance diagrams for network 7, for the CPLEX solution and two different quantum realizations; these can be seen in Fig. 6 (left CPLEX, middle and right two realizations of CQM). We have chosen the line segment between GLC and KZ, offering a good demonstration. (We have introduced a small artificial ‘distance’ between KO and KO(STM) which are contiguous locations for sake of better visibility, hence the horizontal lines in the diagram.) The red dotted lines represent the conflicted situation, and the green solid lines represent the solution. All the three proposed solutions have similar figures of merit, they all provide a valid option to be realized. The conflicts are resolved in somewhat different ways, see e.g. the paths of trains 40150, 5312, and 26103. In details:

- in the CPLEX solution, train 26103 passes first the KTC-CB closure heading for GLC, then 40150 followed by 5312 go in opposite directions,
- in the CQM solution, first realization, 40150 and 5312 pass first the KTC-CB closure and 26103 waits at KTC for them to pass,
- in the CQM solution, second realization, 26103 passes first KTC-CB closure, then 5312 followed by 40150 go in opposite directions.

This results in the following objective  $\times d_{\max}$  values: for CPLEX - 188.75, for CQM first realization - 279 for CQM second realization - 261.5. Although the first solution is optimal, it is reasonable to supply dispatchers with the range of feasible solutions. Hence, these diagrams proved that the CQM hybrid solver can produce usable solutions for railway traffic management.

An additional benefit of the probabilistic nature of the quantum-based method is that it produces different alternatives after each realization run without any modification. These could be offered to the dispatcher in a decision support system as possibilities. The dispatcher’s choice can be influenced by other circumstances not covered by the present model.

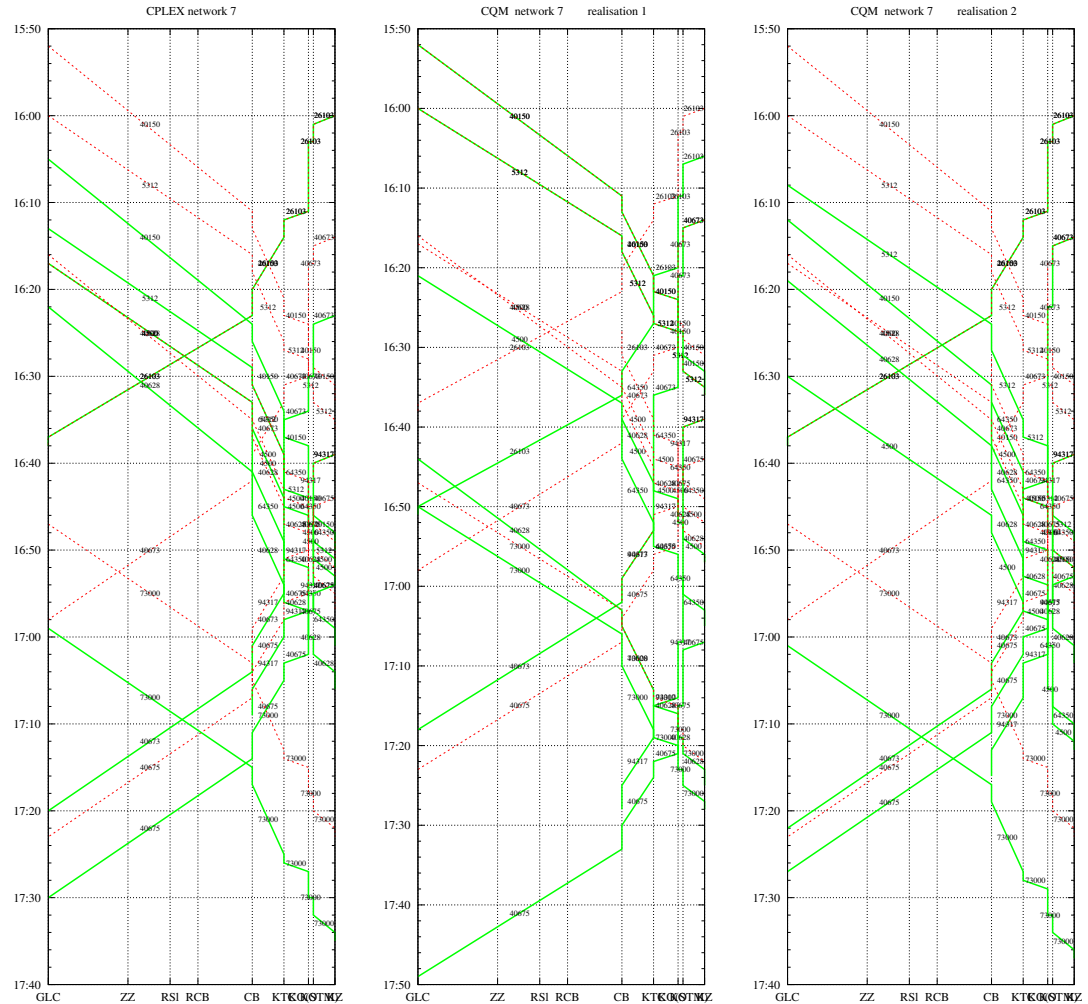


Figure 6: Real-life experiment. Time-distance diagram solution of network 7 CPLEX (left) and two realizations of CQM (middle and right), see Tab. 2. Real-life experiment. Time-distance diagram CQM solution of network 7 (see Tab. 2) first realization. Closures (yielding single-track line) are between CB and KTC as well as between KO(STM) and KZ.